JOURNAL OF Applied Polymer SCIENCE

Special Issue: Bioactive Surface Functionalization

Guest Editor: Prof. Koon Gee Neoh (National University of Singapore)

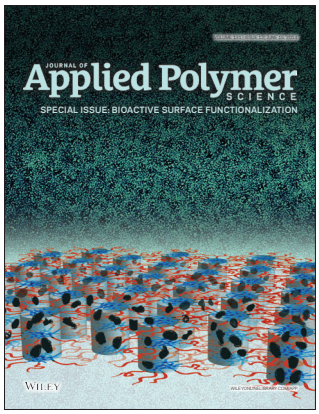

EDITORIAL

Bioactive Surface Functionalization
K. G. Neoh, *J. Appl. Polym. Sci.* 2014, **DOI: 10.1002/app.40607**

REVIEWS

Orthogonal surface functionalization through bioactive vapor-based polymer coatings
X. Deng and J. Lahann, *J. Appl. Polym. Sci.* 2014, **DOI: 10.1002/app.40315**

Surface modifying oligomers used to functionalize polymeric surfaces: Consideration of blood contact applications
M. L. Lopez-Donaire and J. P. Santerre, *J. Appl. Polym. Sci.* 2014, **DOI: 10.1002/app.40328**

Block copolymers for protein ordering
J. Malmström and J. Travas-Sejdic, *J. Appl. Polym. Sci.* 2014, **DOI: 10.1002/app.40360**

RESEARCH ARTICLES

MS-monitored conjugation of poly(ethylene glycol) monomethacrylate to RGD peptides
O. I. Bol'shakov and E. O. Akala, *J. Appl. Polym. Sci.* 2014, **DOI: 10.1002/app.40385**

Synthesis and characterization of surface-grafted poly(*N*-isopropylacrylamide) and poly(carboxylic acid)—Iron particles via atom transfer radical polymerization for biomedical applications
J. Sutrisno, A. Fuchs and C. Evrensel, *J. Appl. Polym. Sci.* 2014, **DOI: 10.1002/app.40176**

Deposition of nonfouling plasma polymers to a thermoplastic silicone elastomer for microfluidic and biomedical applications
P. Gross-Kosche, S. P. Low, R. Guo, D. A. Steele and A. Michelmore, *J. Appl. Polym. Sci.* 2014, **DOI: 10.1002/app.40500**

Regeneration effect of visible light-curing furfuryl alginate compound by release of epidermal growth factor for wound healing application
Y. Heo, H.-J. Lee, E.-H. Kim, M.-K. Kim, Y. Ito and T.-I. Son, *J. Appl. Polym. Sci.* 2014, **DOI: 10.1002/app.40113**

Bioactive agarose carbon-nanotube composites are capable of manipulating brain–implant interface
D. Y. Lewitus, K. L. Smith, J. Landers, A. V. Neimark and J. Kohn, *J. Appl. Polym. Sci.* 2014, **DOI: 10.1002/app.40297**

Preparation and characterization of 2-methacryloyloxyethyl phosphorylcholine (MPC) polymer nanofibers prepared via electrospinning for biomedical materials
T. Maeda, K. Hagiwara, S. Yoshida, T. Hasebe and A. Hotta, *J. Appl. Polym. Sci.* 2014, **DOI: 10.1002/app.40606**

Nanostructured polystyrene films engineered by plasma processes: Surface characterization and stem cell interaction
S. Mattioli, S. Martino, F. D'Angelo, C. Emiliani, J. M. Kenny and I. Armentano, *J. Appl. Polym. Sci.* 2014, **DOI: 10.1002/app.40427**

Microtextured polystyrene surfaces for three-dimensional cell culture made by a simple solvent treatment method
M. E. DeRosa, Y. Hong, R. A. Faris and H. Rao, *J. Appl. Polym. Sci.* 2014, **DOI: 10.1002/app.40181**

Elastic biodegradable starch/ethylene-co-vinyl alcohol fibre-mesh scaffolds for tissue engineering applications
M. A. Susano, I. B. Leonor, R. L. Reis and H. S. Azevedo, *J. Appl. Polym. Sci.* 2014, **DOI: 10.1002/app.40504**

Fibroblast viability and inhibitory activity against Pseudomonas aeruginosa in lactic acid–grafted chitosan hydrogels
A. Espadín, N. Vázquez, A. Tecante, L. Tamay de Dios, M. Gimeno, C. Velasquillo and K. Shirai, *J. Appl. Polym. Sci.* 2014, **DOI: 10.1002/app.40252**

Surface activity of pepsin-solubilized collagen acylated by lauroyl chloride along with succinic anhydride
C. Li, W. Liu, L. Duan, Z. Tian and G. Li, *J. Appl. Polym. Sci.* 2014, **DOI: 10.1002/app.40174**

Collagen immobilized PET-g-PVA fiber prepared by electron beam co-irradiation
G. Dai, H. Xiao, S. Zhu and M. Shi, *J. Appl. Polym. Sci.* 2014, **DOI: 10.1002/app.40597**

Journal of Applied Polymer Science

Synthesis and Characterization of Surface-Grafted Poly(*N*-isopropylacrylamide) and Poly(carboxylic acid)—Iron Particles via Atom Transfer Radical Polymerization for Biomedical Applications

Joko Sutrisno,[1] Alan Fuchs,[1] Cahit Evrensel[2]
[1]Chemical Engineering Department, University of Nevada, Reno, Nevada
[2]Mechanical Engineering Department, University of Nevada, Reno, Nevada
Correspondence to: A. Fuchs (E-mail: afuchs@unr.edu)

ABSTRACT: This research relates to the preparation and characterization of surface grafted poly(*N*-isopropylacrylamide) and poly(carboxylic acid)–micron-size iron particles via atom transfer radical polymerization (ATRP). The surface grafted polymers–iron particles result in multifunctional materials which can be used in biomedical applications. The functionalities consist of cell targeting, imaging, drug delivery, and immunological response. The multifunctional materials are synthesized in two steps. First, surface grafting is used to place polymer molecules on the iron particles surface. The second step is conjugation of the bio-molecules onto the polymer backbone. Fourier transform infrared (FTIR) spectroscopy and scanning electron microscopy were used to confirm the presence of polymers on the iron particles. The thickness of the grafted polymers and glass transition temperature of the surface grafted polymers were determined by transmission electron microscopy (TEM) and differential scanning calorimetry (DSC). The covalent bond between grafted polymers and iron particles caused higher glass transition temperature as compared with nongrafted polymers. The ability to target the bio-molecule and provide fluorescent imaging was simulated by conjugation of rat immunoglobulin and fluorescein isothiocyanate (FITC) labeled anti-rat. The fluorescence intensity was determined using flow cytometry and conjugated IgG-FITC anti-rat on iron particles which was imaged using a fluorescence microscopy. © 2013 Wiley Periodicals, Inc. J. Appl. Polym. Sci. **2014**, *131*, 40176.

KEYWORDS: biomedical applications; biomaterials; differential scanning calorimetry (DSC); surfaces and interfaces; properties and characterization

Received 14 June 2013; accepted 7 November 2013
DOI: 10.1002/app.40176

INTRODUCTION

The applications of iron particles, with various sizes, compositions, and shapes, in the biomedical fields have attracted worldwide attention during the past few years.[1–3] Nonfunctionalized iron particles only have limited applications. However, surface modification provides a wide range of applications, such as cell targeting, biomolecule separation, hyperthermia, magnetic resonance imaging (MRI), drug delivery, and magneto-immune response. The iron particles surface modification can be done by coating with biocompatible inorganic (e.g., silica oxide and gold) or organic materials. The organic layer on the surface of the iron particles can be adjusted from a few layers of atoms up to the nanometer scale by coating with small organic molecules or polymers. The surface functionalized iron particles with thin organic layers are commercially available, such as Feridex (dextran associated iron oxide) for contrast enhanced MRI,[4] and are carboxylic acid functionalized for bio-molecule separations.[5] For hyperthermia applications, the heat generated from the iron particles by magnetic hysteresis effects result from on-off switching of the magnetic field.[1–3] Hence, high magnetic saturation properties of the iron particles must be maintained if the particles are subjected to surface coating.

The stimuli from external conditions, such as temperature and pH, which result in a molecular property change, can be used to create a stimuli-responsive polymer. For instance, poly(*N*-isopropylacrylamide) (poly(NIPAAm)) is a thermo-responsive polymer that exhibits a reversible property change in hydropobic-hydrophilicity when it is exposed to a temperature gradient. Poly(NIPAAm) dissolved in aqueous media is well known to experience a lower critical solution temperature (LCST) at approximately 32°C.[6] In addition, the well defined copolymer architecture of NIPAAm has been investigated and provides an adjustable thermal phase change.[7] The controlled phase change of poly(NIPAAm) based on thermal stimulation

allows controlled drug delivery. The carboxylic acid moiety can be used to bind the bio-molecules through the carbodiimide linkage. A copolymer of poly(carboxylic acid) with poly(NIPAAm) can be used as a multifunctional polymer for drug delivery, targeting specific cells, and bio-molecules separation.

Controlled radical polymerization [e.g., atom transfer radical polymerization (ATRP)] is one of the techniques used to synthesize copolymers with well defined architecture. ATRP was developed by Matyjaszewski et al.[8] and offers advantages for synthesis, such as a wide range of monomers, mild and elevated polymerization temperatures, narrow polydispersity index, controlled topologies, functionalities, and composition of polymers.[9–17] ATRP involves redox reactions between the organic halide initiator, metal halides (e.g., copper bromide) as a catalyst, and a ligand to improve the solubility of metal salts in the organic reaction system.[9] The copper bromide releases electrons and initiates the organic halide initiator. The active radical initiates the monomer. The polymer is terminated and endcapped by the halide group in the termination stage which may be used further as a macroinitiator.[9] The thermo-responsivity of poly(*N*-isopropylacrylamides-*co*-*N*-hydroxymethylacrylamide) in water has been developed using ATRP.[7] The use of ATRP to synthesize temperature- and pH-sensitive copolymers of NIPAAm and sodium acrylate has been investigated.[18] Poly(NIPAAm) has been successfully coated on the surface of silica nanoparticles and iron nanoparticles.[8,13,14]

In this research, a synthesis technique and characterization of multifunctional materials based on micron-size iron particles is reported. This approach is not only provide drug storage and release capability from thermo-responsive poly(NIPAAm), but also offers targeting and imaging functionalities through carboxylic (AA) functional groups. In addition, the iron particles provide a magneto-immune response via exposing in the magnetic field. Multifunctional materials were prepared using two steps. First, surface grafting of poly(NIPAAm-*co*-AA) on iron particles using ATRP at mild temperature in the presence of copper (II) bromide was carried out. Second, conjugation of rat immunoglobulin as a bio-molecule model for targeting FITC anti-rat was accomplished. The glass transition temperature of grafted polymers was investigated and found to be higher than for non-grafted polymers because of a covalent bond formed between the polymer chain and the inorganic substrate. To the best of our knowledge, this is the first time that the grafting technique of poly(NIPAAm-*co*-AA) using ATRP on the micron-size iron particles was used to prepare multifunctional materials.

EXPERIMENTAL

Materials

The following materials were used: carbonyl iron powder CN (3–7 μm, BASF), methanol (Aldrich), ethanol (AAPER), 1-octyl-2-pyrrolidone (OP) (Aldrich), copper (I) bromide (CuBr) (Aldrich), copper (II) bromide ($CuBr_2$) (Aldrich), sparteine (Aldrich), toluene (Aldrich), 2–4(-chlorosulfonylphenyl)-ethytrichlorosilane (CTCS) (Gelest Inc.), dimethylformamide (DMF) (Aldrich), dimethylsulfoxide (DMSO) (Aldrich), *N*-isopropylacrylamide (NIPAAm) (Aldrich), sodium acrylate (Aldrich), micro iron particles functionalized carboxylic acid (Polysciences, Inc.), ChromPure rat immunoglobulin (IgG), whole molecule (Jackson ImmunoResearch Laboratories, Inc.), fluorescein (FITC)-conjugated affinipure F(ab')2 fragment goat anti-rat IgG (Jackson ImmunoResearch Laboratories, Inc.), fetal bovine serum (FBS) buffer, PolyLink protein coupling kit for COOH microspheres (Polysciences, Inc.): Polylink coupling buffer (50 m*M* MES, pH 5.2, 0.05% Proclin® 300), Polylink wash/storage buffer (10 m*M* Tris, pH 8.0, 0.05% bovine serum albumin, 0.05% Proclin® 300), and Polylink EDAC (carbodiimide). Benchmark iron particles functionalized carboxylic acid (benchmark Fe-COOH) (Polysciences, Inc.). NIPAAm was purified by recrystallization in methanol.

Synthesis

Iron Particles Surface Grafting via ATRP. ***Surface grafting - poly(N-isopropylacrylamide).*** The procedure for immobilization of a surface initiator onto iron particles was as follows[19]: Three hundred grams (300 g) of iron particles were washed with distilled water and ethanol, respectively. Then, the iron particles were dried in a vacuum oven at 50°C for 8 h and cooled down. Iron particles and 100 g toluene were added to the reaction flask. Five grams of CTCS were added to the reactor and the reaction was carried out at 85°C for 24 h under nitrogen. The mixture was then filtered and washed with methanol in order to remove excess CTCS. The residual (Fe-CTCS) was dried in a vacuum oven at 40–50°C for 24 h.

The procedure for surface coating of iron particles using poly(-NIPAAm) via ATRP was as follows: 50 g functionalized Fe-CTCS, 0.06 g CuBr, 0.03 g $CuBr_2$, 0.06 g Spartein, and 14.2 g NIPAAm monomer, and 60 mL DMSO were added to the reaction flask. The mixture was reacted at 25–30°C for 24 h under nitrogen. Finally, the mixture was filtered, washed several times with ethanol and dried in a vacuum oven at 40–50°C prior to use.[19] The ATRP mechanism for surface polymerization is shown in Figure 1.

Surface grafting poly(acrylic acid). The procedure for surface coating iron particles using poly(AA) via ATRP was as follows: 50 g functionalized Fe-CTCS, 0.06 g CuBr, 0.03 g $CuBr_2$, 0.06 g Spartein, and 9.4 g sodium acrylate monomer, and 60 mL DMSO were added to the reaction flask. The mixture was reacted at 25–30°C for 24 h under nitrogen. Finally, the mixture was filtered, washed several times with ethanol and dried in a vacuum oven at 40–50°C prior to use.[19] The substitution of sodium with hydrogen atom was accomplished by dispersing 1 g surface coated poly(sodium acrylate)–iron particles in 40 mL mixture of water:ethanol (50:50%v/v). The suspension was then sonicated for 10 min. The iron particles was separated, washed with mixture of water : ethanol, and dried under vacuum oven at 60°C under nitrogen environment. The mechanism of substitution of sodium with hydrogen atom is shown in Figure 2.

Surface grafting poly(N-isopropylacrylamide-co-acrylic acid). The procedure for surface coating iron particles using poly(NIPAAm-*co*-AA) via ATRP were as follows: 40 g functionalized Fe-CTCS, 0.06 g CuBr, 0.03 g $CuBr_2$, 0.06 g Spartein, and 9.4 g sodium acrylate and 11.3 g NIPAAm monomers, and 60 mL OP were added into reaction flask. The mixture was reacted at 25–30°C for 48 h under nitrogen. Finally, the mixture was filtered,

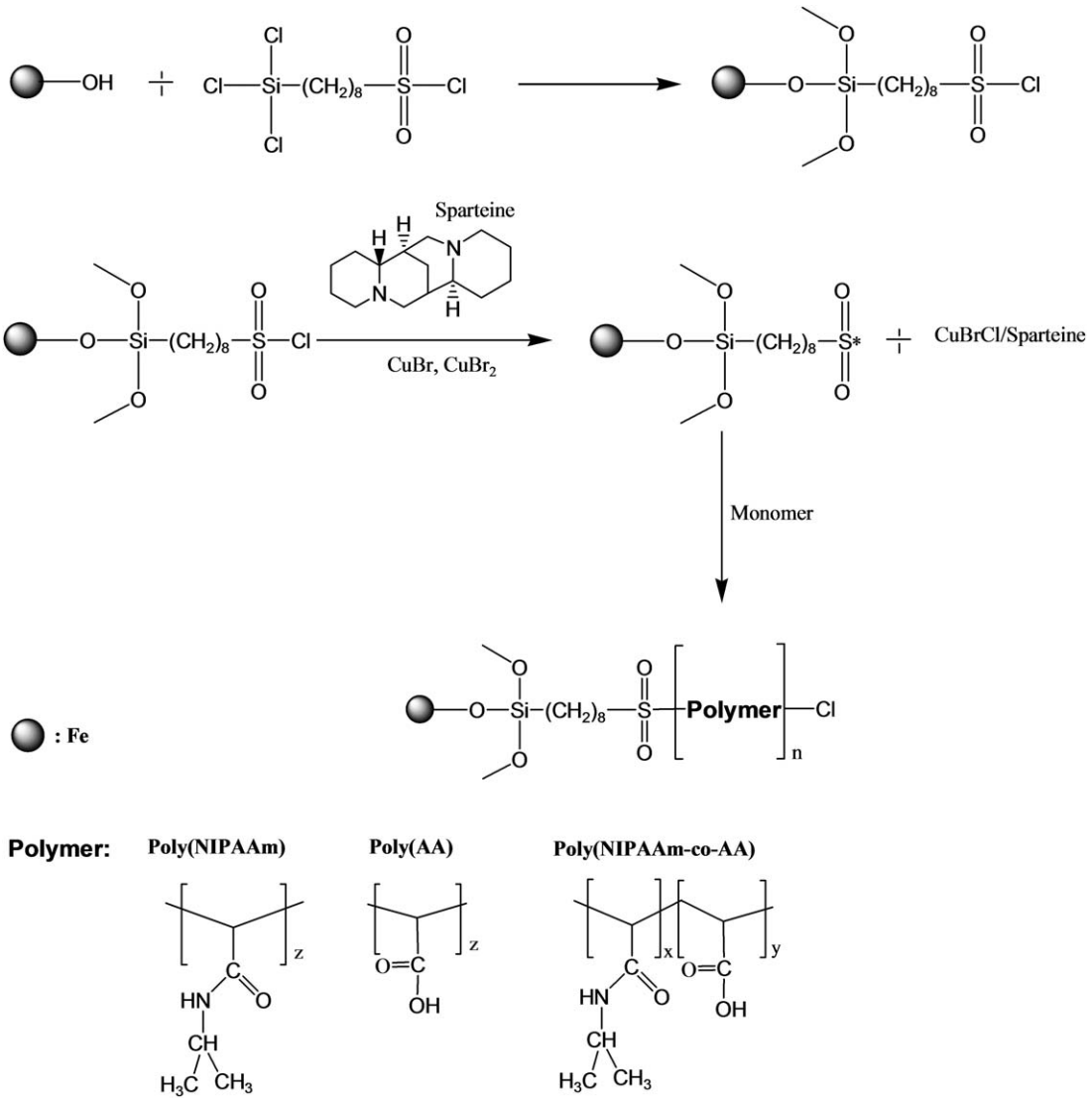

Figure 1. Surface polymerization of various polymers: poly(NIPAAm), poly(AA), and poly(NIPAAm-co-AA) on the iron particles using ATRP technique.

washed several times with ethanol, and dried in a vacuum oven at 40–50°C prior to use.[19] The substitution of sodium with hydrogen atom was accomplished by described method in previous section. The molecular weight of poly(NIPAAm-*co*-AA) was determined by setting up another batch of reaction without the presence of iron particles while maintaining the same composition for each reactant and DMSO was used as a solvent.

Conjugation of Rat Immunoglobulin onto Iron Particles. Surface coated iron particles (12.5 mg), that contain and acrylic acid functional group (poly(NIPAAm-co-AA), poly(AA)), were weighed and placed into a vial. Polylink coupling buffer (0.4 mL) was added into the vial and the suspension was mixed for 1 min. The suspension was then separated using a magnet to attract the iron particles and supernatant was then removed. This step was repeated three times. Iron particles were

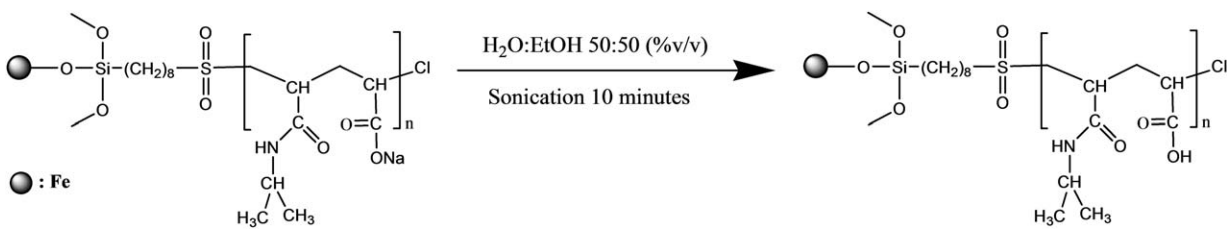

Figure 2. The mechanism of substitution of sodium with hydrogen atom.

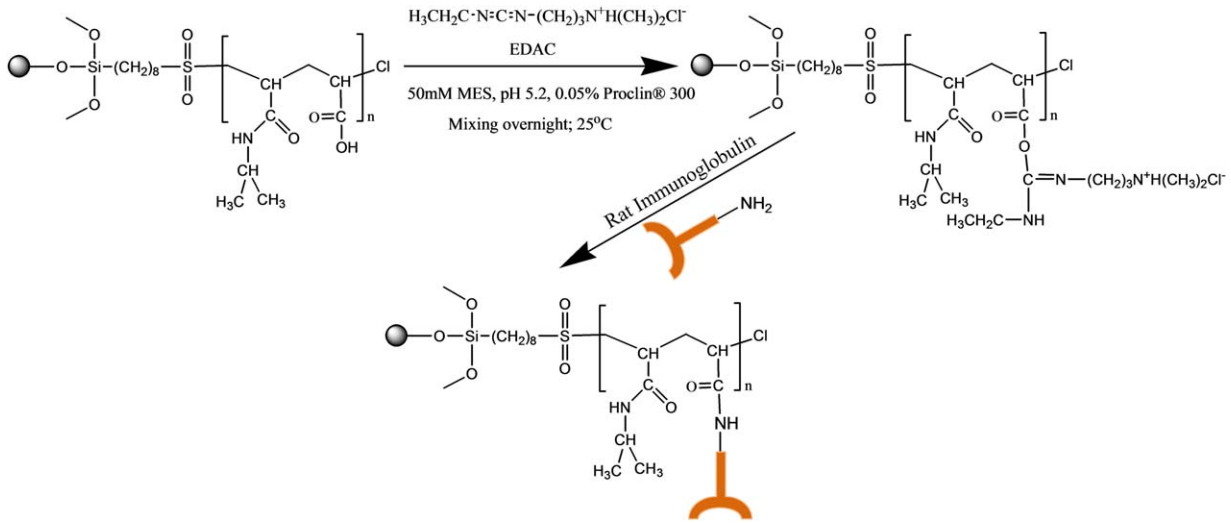

Figure 3. The mechanism of conjugation of IgG onto polymer coated iron particles. [Color figure can be viewed in the online issue, which is available at wileyonlinelibrary.com.]

suspended in 0.17 mL Polylink coupling buffer and 20 μL of the EDAC solution (200 mg/mL) was added. Totally, 200 μg ChromPure rat immunoglobulin (IgG) was added to the suspension and was mixed gently for 8 h at room temperature. After the incubation process, the iron particles were separated using a magnet and washed twice with 0.4 mL Polylink wash/storage buffer to remove the excess of IgG. The conjugated IgG-iron particles were stored in 1 mL Polylink wash/storage buffer prior to use. The mechanism of conjugation of IgG onto polymer-coated iron particles is shown in Figure 3.

Conjugation of FITC Anti-Rat onto Iron Particles. Fifty (50) μL of conjugated IgG–polymer-coated iron particles suspension (12.5 mg/mL) were transferred into a vial and washed with 2 mL FBS buffer. The suspension was centrifuged at 1200 rpm for 10 min. The supernatant was then removed. The conjugated IgG–polymer coated iron particles were then resuspended in 100 μL FBS buffer and mixed gently. FBS (0.8 mL) buffer was injected into FITC anti-rat in a bottle and mixed for 1 min to dissolve the powder completely. The solution (100 μL) was transferred into a vial and diluted 100 times. Diluted FITC (10 μL) anti-rat solution was added to conjugated IgG–polymer-coated iron particles suspension and mixed for 1 min. The mixture was incubated for 30 min at room temperature. The excess FITC anti-rat was removed by washing with FBS buffer. The mechanism of conjugation of FITC–anti rat onto polymer-coated iron particles is shown in Figure 4.

Characterization

Proton Nuclear Magnetic Resonance (^{1}H-NMR). The polymerized NIPAAm-*co*-AA was characterized using ^{1}H-nuclear magnetic resonance spectroscopy. The polymer was synthesized by setting up a batch reaction which has a similar composition to the surface polymer without the presence of iron particles. The synthesized polymer was isolated in hot hexane and washed several times. The NMR spectrum was recorded using Agilent NMR 400 (^{1}H at 400 MHz) in DMSO-d_6 at 25°C.

Gel Permeation Chromatography (GPC). The molecular weight of poly(NIPAAm-*co*-AA) was determined using a Shimadzu LC-20AD pump, CBM-20A controller, DGU-20A$_3$ degasser, RID-10A refractive index detector, CTO-20AC column oven, and single Phenogel 5 μm 10^4 angstrom column which has an effective molecular weight of 5,000–500,000 g/mol. The GPC column was calibrated against nearly monodisperse polystyrene standards purchased from Sigma Aldrich (certified by Scientific Polymer Product, Inc.). The mobile phase was *N,N*-

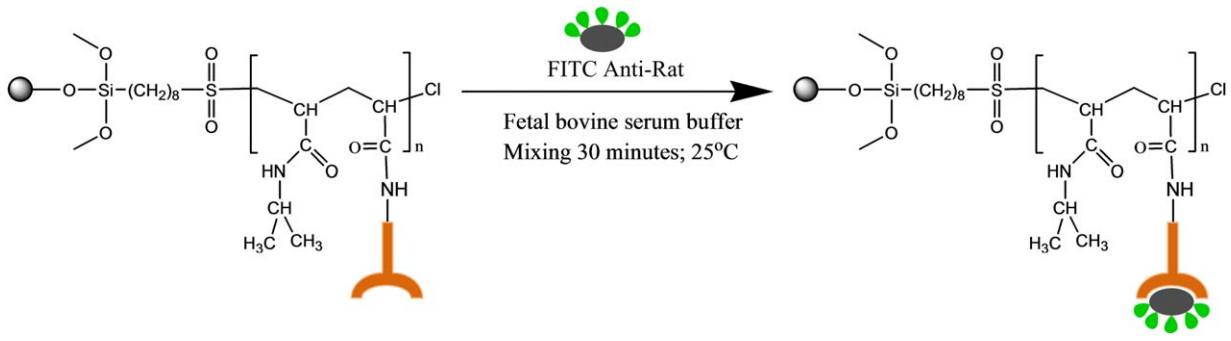

Figure 4. The mechanism of conjugation of FITC–anti rat onto polymer coated iron particles. [Color figure can be viewed in the online issue, which is available at wileyonlinelibrary.com.]

dimethylformamide 99.9% HPLC grade with a flow rate of 0.8 mL/min, column temperature was set at 35°C, and 20 μL of polymer solution was injected through column. Molecular weight averages and polydispersity index (M_w/M_n) of the polymer was calculated by using LabSolutions software. The molecular weight of the polymer coating on the surface of the iron particles was determined by reaction of a similar composition without the presence of iron particles. The poly(NIPAAm-*co*-AA) was isolated in hot hexane and washed several times.

Fourier Transform Infrared (FTIR) Spectroscopy. The spectra of uncoated iron, immobilized surface initiator iron particles, and grafted poly(NIPAAm-*co*-AA)/iron particles were analyzed using Perkin-Elmer Spectrum 100 Fourier transform infra red spectroscopy. The samples were dried in a vacuum oven at 60°C for 24 h and stored in a desiccator prior to characterization. The particles were uniformly mixed with KBr powder at a weight ratio of 1 : 50, before mechanically pressing them to form moisture-free KBr pellets. The spectra were scanned and recorded from 4000 cm^{-1}−400 cm^{-1} at room temperature with a resolution of 4 cm^{-1}.

Differential Scanning Calorimetry (DSC). Perkin-Elmer Pyris-1 DSC was used to characterize the thermal properties of the grafted polymers on the iron particles surfaces. All samples were dried in a vacuum oven at 60°C for 24 h and stored in a desiccator prior to characterization. Two pans were placed in the DSC sample holder, one containing the sample and the other holding a reference. Then, surface coated iron particles were weighed and placed in the DSC sample pan. The sample was then scanned from 50°C to 350°C with a heating rate of 10°C/min. This characterization was done under nitrogen purge of 20 mL/min.

Scanning Electron Microscopy—X-ray Energy Dispersive Spectrum (SEM-XEDS). SEM-XEDS samples were prepared by placing surface grafted polymers–iron particles onto carbon tapes attached to an aluminum SEM sample holder. A thin layer coating of platinum was applied to the mounted samples using an argon plasma sputtering system. The platinum coating was done at an approximate rate of 25–30 nm/min with 85mA. Hitachi S-4700 equipped with an Oxford EDS System was used for characterization of surface morphologies of grafted polymers–iron particles, and chemical analysis of surface-coated iron particles. The samples were magnified from 800X to 35,000X at an accelerating potential of 20kV. EDS microanalysis was performed on the samples at magnifications ranging from 10,000X to 30,000X and an accelerating potential of 20 kV.

Transmission Electron Microscopy (TEM). The polymer coating thickness was characterized using an FEI Titan 80–300 TEM system equipped with an 80–300 Kv field emission electron source, 0.8 Å resolution in TEM mode and 1.4 Å STEM resolution, and bright field/dark field and high angle annular dark field (HAADF) STEM imaging capability. The polymer surface-coated iron particles were dispersed in ethanol and drop cast on a copper TEM grid.

Flow Cytometry. The fluorescent intensity of conjugated FITC anti-rat with IgG–polymer-coated iron particles was characterized using a flow cytometer BD LSR II equipped with four lasers (405 nm, 488 nm, 561 nm, and 640 nm) with a total of 18 fluorescence detectors. The sample was prepared by dispersing the conjugated FITC anti-rat with IgG–polymer-coated iron particles in FBS buffer, and nonconjugated FITC anti-rat with IgG–polymer-coated iron particles were used as a control. The suspension was analyzed at room temperature and the flow rate was adjusted (12, 35, and 60 μL/min) depending upon sample concentration.

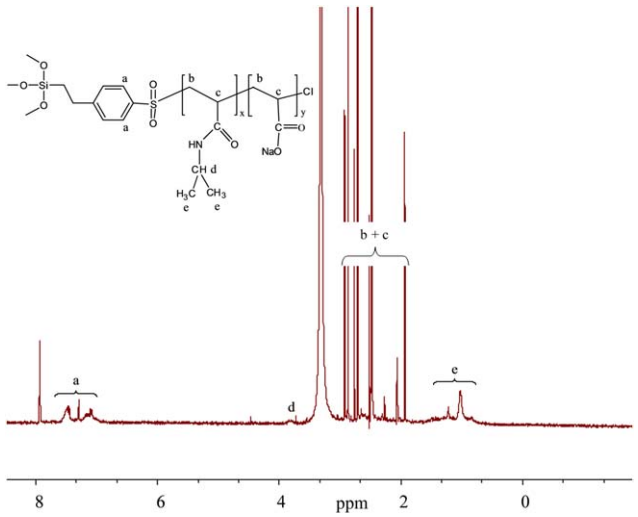

Figure 5. ^{1}H-NMR spectra of poly(NIPAAm-*co*-AA)in DMSO-d_6 at 25°C. [Color figure can be viewed in the online issue, which is available at wileyonlinelibrary.com.]

Fluorescent Microscopy. The fluorescent images of conjugated FITC anti-rat with IgG–polymer-coated iron particles was taken using Zeiss LSM510 confocal and fluorescence microscope. The suspension of non- and conjugated FITC anti-rat with IgG–polymer-coated iron particles was dispersed onto a microscope slide and put on the sample holder. The image was taken at 40X magnification in two different modes; differential interference contrast (DIC) and fluorescence.

RESULT AND DISCUSSION

^{1}H-NMR and Gel Permeation Chromatography (GPC)

The presence of NIPAAm-*co*-COONa functional group is identifed by ^{1}H-NMR spectra. The signal peaks at ∼1.0 ppm represented *iso*-propyl CH_3 groups of NIPAAm. The chemical shifts of CH-Me_2 protons adjacent to the amine moiety of NIPAAm were shown by the peaks at about 3.9 ppm.[18,20–23] The multiple peaks at approximately 2.0–3.0ppm were associated with the methyl group on the main chain of copolymer.[21] The broad peaks at approximately 3.3–3.5ppm were derived from the CH_2 proton from CTCS.[22] The proton chemical shift at 7.1 ppm and 7.4 ppm derived from the methylene proton in the benzene ring of CTCS.[21] In addition, Figure 5 shows that disappearance of the vinyl group chemical shift at approximately 5.5–6.5 ppm which confirmed that the polymer was relatively pure after 48 h of reaction at room temperature and with removal of the impurities by passing the solution through an alumina column. The polymerization of NIPAAm-*co*-COONa at mild temperature

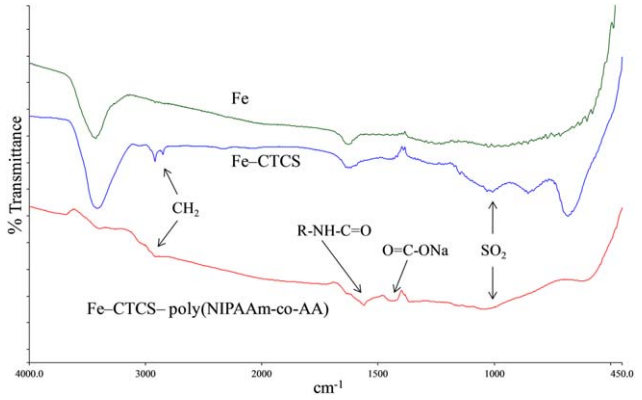

Figure 6. FTIR spectra of iron particles (Fe), immobilized CTCS on iron particles (Fe–CTCS), and grafted poly(NIPAAm-*co*-AA) on iron particles (Fe–CTCS– poly(NIPAAm-*co*-AA)). [Color figure can be viewed in the online issue, which is available at wileyonlinelibrary.com.]

in dimethylsulfoxide using ATRP resulted in a copolymer with a molecular weight (M_w) of 5.95 x 10^4 g/mol with a polydispersity index of 1.1. Synthesized poly(NIPAAm-*co*-COONa) has a high molecular weight and narrow dispersity index which results from the presence of copper (II) bromide. According to the literature,[10,23,24] copper (II) bromide played a role in the control of the kinetics of reaction by reducing the growing chain rate which converts the propagating polymer chain into a dormant species.

Fourier Transforms Infrared (FTIR) Spectroscopy

Figure 6 shows the spectra of uncoated iron particles (Fe), immobilized CTCS on iron particles (Fe–CTCS), and grafted poly(NIPAAm-*co*-AA) on iron particles [Fe–CTCS–poly(NIPAAm-*co*-AA)]. The hydroxyl stretching vibration was represented by a broad band at 3500–3400 cm^{-1} in the spectrum of Fe and Fe–CTCS,[24,25] and the band at 2950–2850 cm^{-1} corresponds to C—H bond stretching and bending of the surface initiator methyl group in the spectrum of Fe–CTCS and grafted poly(NIPAAm-*co*-AA).[26–28] The presence of carboxyl stretching vibration and N—H-bending vibration from the amide group of NIPAAm was shown by a broad peak at 1500–1650 cm^{-1} in the spectrum of grafted poly(NIPAAm-*co*-AA).[27,29–31] According to the literature,[28,30] the contribution of carboxylate from sodium acrylate was indicated by the peak shift at 1425–1450 cm^{-1} in the spectrum of grafted poly(-NIPAAm-*co*-AA).[28] The stretching bond of SO_2 which occurred at peaks at 1000–1250 cm^{-1},[24,32,33] in the spectrum of Fe–CTCS and grafted poly(NIPAAm-co-AA), confirmed the immobilized surface initiator. In addition, the C—Cl bond from the surface initiator was shown at peaks 800–600 cm^{-1}.[24,26,32]

The presence of NIPAAm and AA functional groups provides the drug delivery and targeting capability. Poly(NIPAAm) exhibits a low critical solution temperature (LCST) at 32°C.[22] This thermal responsive property of the polymer is suitable for the drug storage and release functions. The phase transition of poly(NIPAAm) can be varied by copolymerizing with another monomer. The copolymer of poly(NIPAAm), with a different ratio of monomers, results in a wide range of phase transitions reported.[7] The drug uptake and release capability of poly(NIPAAm), and the process of binding biotin-streptavidin bio-molecules through the poly(AA) functional group was investigated.[34–36]

Differential Scanning Calorimetry (DSC)

The presence of polymer on the surface of the iron particles and the thermal transition temperature of the grafted polymers has been analyzed using differential scanning calorimetry (DSC). From DSC, it is possible to obtain information about the thermal properties of polymers, such as heat capacity (thermodynamic Cp) which relates to molecular vibration and glass transition temperature (T_g) which also relates to molecular rotation. The change in heat supplied (heat flow endothermic up–*Y*-axis) signifies the individual thermal transition temperature of each polymer. The glass transition temperature of the polymer grafted onto the surface of the iron particles was measured in the experiments. Then, the thermal transition temperatures from the experiments were compared with available data from the literature which are found for nongrafted polymers. The decreased mobility of the polymer due to the covalent bonding on the surface of the iron particles which may result in the differences in glass transition temperatures between literature and experiment. The covalent bonds between the polymer and the surface of particles causes higher energy requirements to achieve the glassy state of the polymer before reaching the glass transition temperature. In addition, the hydrogen bonding among the NIPAAm-NIPAAm, AA-AA, and NIPAAm-AA functional groups may contribute to the increase in glass transition temperatures.[29,37] The hydrogen bond scheme is shown in Figure 7. The results were in agreement with literature[15] which compared the thermal transition temperature between polystyrene and grafted polystyrene onto the surface of silica oxide. The literature value was ~20°C higher for the grafted polymer. The glass transition temperature of a variety of polymers is listed in Table I and the DSC results for surface grafted polymers are shown in Figure 8.

Scanning Electron Microscopy—X-ray Energy Dispersive Spectrum (SEM-XEDS) and Transmission Electron Microscopy (TEM)

Information about surface grafted polymer morphology and thickness can be obtained by SEM and TEM. Samples were

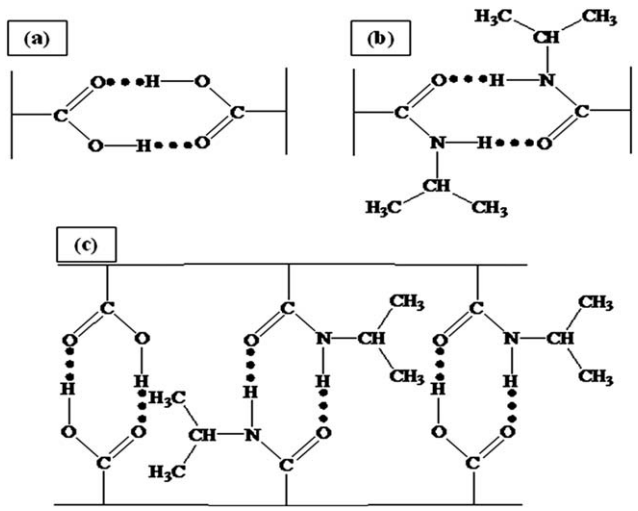

Figure 7. The hydrogen bond of: (a) poly(AA), (b) poly(NIPAAm), and (c) poly(NIPAAm-*co*-AA).

Table I. T_g of Grafted Polymer and Literature

Grafted polymers	Experiment (°C)	Literature (°C)
Poly(AA)	140.4	110[38]
Poly(NIPAAm)	151.5	135[39]
Poly(NIPAAm-co-AA)	190.9	170[40]

subjected to platinum sputter coating, prior to the SEM observation, to distribute the effects of heating, to increase the intensity of secondary and back-scattered electrons at high resolution, and to prevent the charging of the organic compound excessively. The electron beam acceleration voltage needs to be appropriately selected to avoid thermal degradation of polymer coating and to achieve accurate elemental quantification.

Figure 9 shows the individual uncoated iron particles and surface grafted surface poly(AA), poly(NIPAAm), and poly(NIPAAm-*co*-AA). The grafted polymers were coated on the individual iron particles, which was an advantage of ATRP, because it is a controlled living polymerization. In addition, a surface initiator, which was silane based, covalently bonds the grafted polymers on the iron surface and a narrow molecular weight distribution of the polymer results.[9–11,13,14,16] Hence, it was possible to control the coating thickness on the particle surfaces. The thickness of surface grafted poly(NIPAAm-*co*-AA) on the particles was measured by TEM image and shown in Figure 10. From the TEM image of surface grafted poly(NIPAAm-*co*-AA), the thickness of coating was in the range of 20–50 nm.

The surface coated polymers are not magnetizeable materials but because they are thin films, the effect on decreasing magnetic saturation of the iron particles can be considered negligible. Polymer surface coatings on similar iron particles, with coating thickness of 50–100 nm, have been done by our group.[41] It has been shown that the magnetic effect only decreased less than 5%. It is also in agreement in the reported literature.[42] The micron-size iron particles produce higher magnetic saturation than nanometer size particles which resulted in a stronger magnetic effect on the micro-particles. The magnetic effect on the micron-size particles was highly dependent on the particle diameter, concentration, and applied magnetic field. At equal concentrations and applied magnetic fields, larger iron particles resulted in a higher magnetic effect.[43] Similarly, a higher concentration of iron particles and higher applied magnetic field yielded a higher MR effect.[43] According to the literature,[12] the viscoelastic effect (in terms of shear yield stress) of the magnetic fluids, containing iron particles (80 wt %) dispersed in fluid media, increased significantly from less than 1,000 Pascal to 30,000 Pascal when the fluid was exposed to 0 Tesla to 0.529 Tesla magnetic fields. The controllable viscoelastic properties of the magnetic fluid may offer advantages for

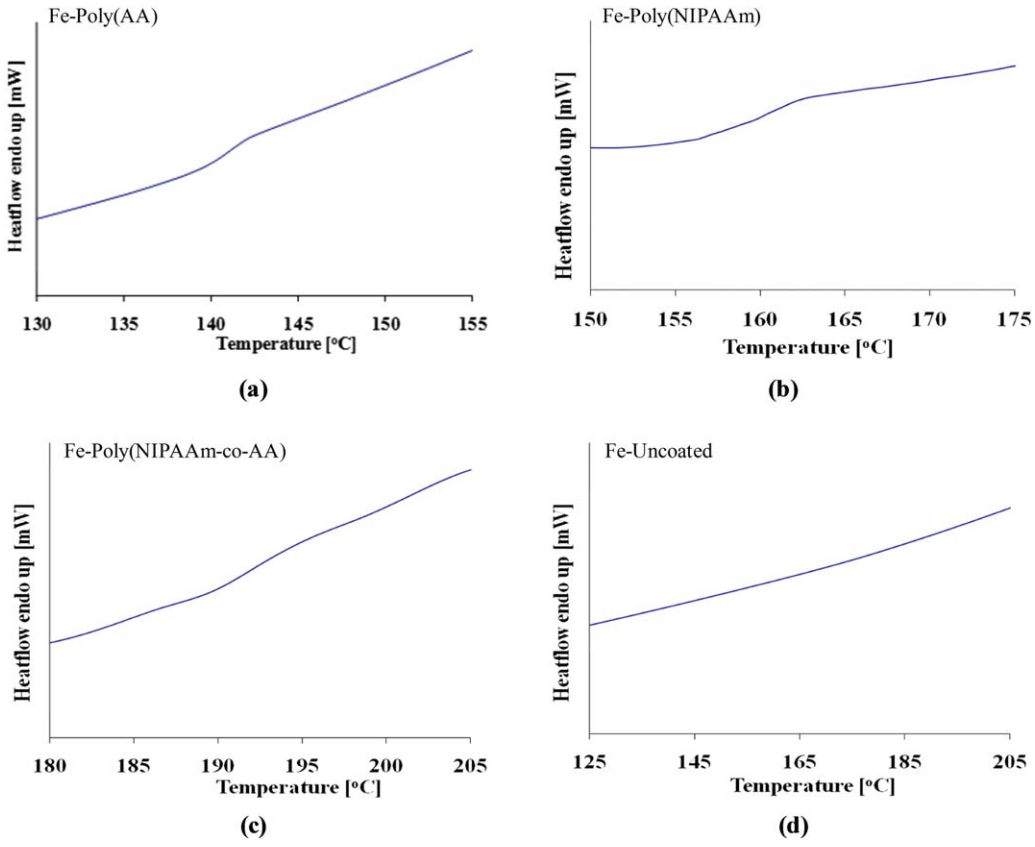

Figure 8. DSC thermograms of surface grafted polymers: (a) Fe–Poly(AA), (b) Fe–Poly(NIPAAm), (c) Fe–Poly(NIPAAm-*co*-AA), and (d) Fe–Uncoated. [Color figure can be viewed in the online issue, which is available at wileyonlinelibrary.com.]

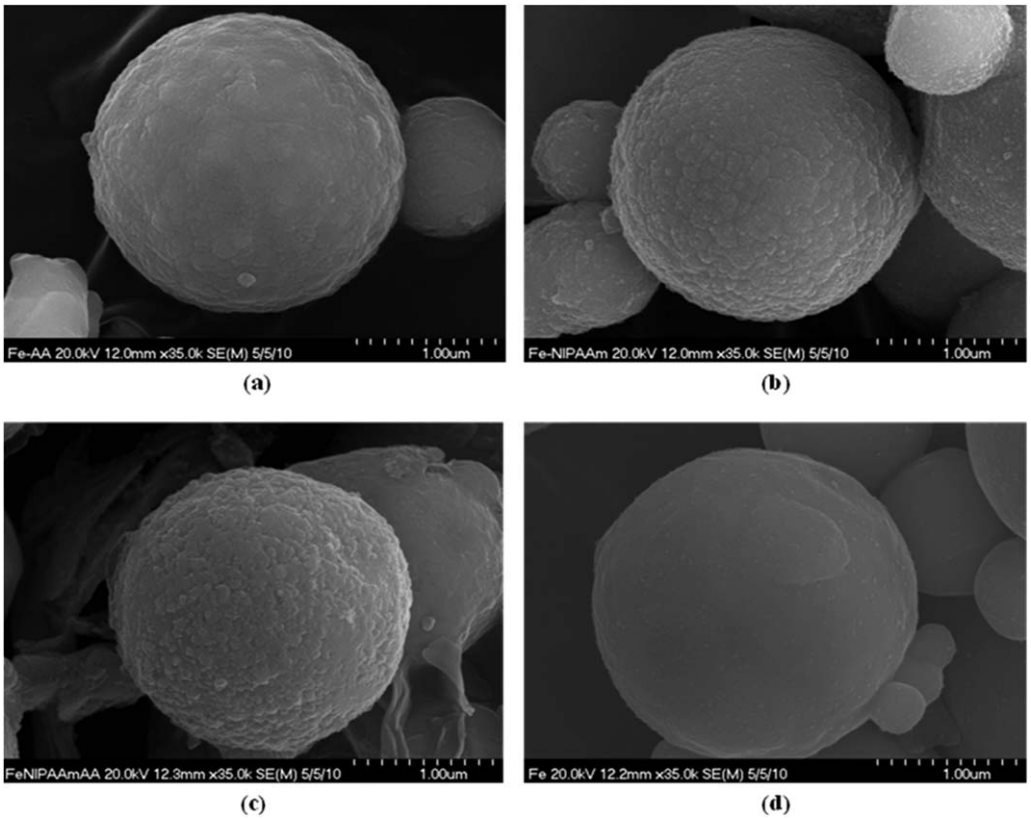

Figure 9. SEM images of iron particles: (a) Fe–poly(AA), (b) Fe–Poly(NIPAAm), (c) Fe–poly(NIPAAm-*co*-AA), and (d) Fe–uncoated.

inducing an immune response by cell destruction for *in-vivo* applications after magnetic injection and exposure to magnetic fields.

The quantitative elemental analysis of x-ray energy dispersive spectroscopy was mainly used for confirming the presence of carbon atoms on the grafted polymers. From elemental analysis, the weight percentage of iron atoms decreased when the iron particles were coated with polymers. On the other hand, the number of carbon atoms increased after a surface coating was applied. As a result, the elemental analysis confirms the surface grafting of poly(AA), poly(NIPAAm), and poly(NIPAAm-*co*-AA) on the iron particles via ATRP at room temperature was a viable technique to graft covalently bonded polymers on the inorganic substrate. The weight percentage of each element for uncoated iron particles, and the grafted poly(AA),

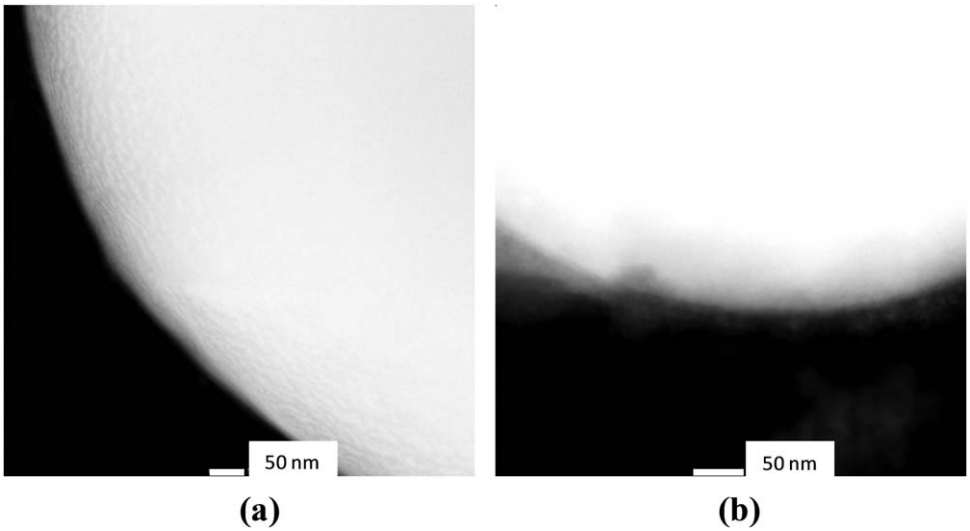

Figure 10. TEM images of iron particles: (a) Noncoated, (b) Poly(NIPAAm-*co*-AA).

Table II. Element Analysis from X-ray Energy Dispersive (X–EDS)

	Weight %			
Element	Fe-uncoated	Fe-poly(AA)	Fe-poly(NIPAAm)	Fe-poly(NIPAAm-co-AA)
Fe	100.00	2.31	4.95	5.39
C	-	97.69	95.05	94.61
Total	100.00	100.00	100.00	100.00

poly(NIPAAm), and poly(NIPAAm-*co*-AA) on the surface of iron particles from x-ray energy dispersive spectrograms is shown in Table II. The X–EDS spectrograms of iron particles, and polymer-coated iron particles are shown in Figure 11.

Fluorescent Microscopy and Flow Cytometry

A model of the targeting functionality of polymer surface coated iron particles containing acrylic acid, was provided by conjugation of rat immunoglobulin. FITC anti-rat was used as a target cell model. Once the FITC anti-rat was conjugated, the polymer surface coated iron particles have an additional functionality which was used for imaging. Flow cytometry was used for identifying the presence of fluorescent labeled microparticles. In addition, the dual imaging (DIC) and fluorescence modes were beneficial methods used to support and image the conjugated IgG and FITC anti-rat on the surface coated iron particles. In the fluorescence imaging process, IgG-conjugated surface-coated iron particles were used as a control. Figure 12 shows the microscope images of iron particles that contain the acrylic acid functional group; Fe–poly(NIPAAm-*co*-AA) denoted as *a*, Fe–poly(AA) denoted as *b*, and Fe-COOH denoted as *c*.

The acrylic acid functional group from the coated polymer on the surfaces provided a robust platform for covalently bonding rat IgG with iron particles. The conjugated IgG could be detected by conjugation of FITC anti-rat. By comparing images of a_1 (control, nonfluorescence labeled) and a_2, Fe–poly(NIPAAm-*co*-AA)/IgG/FITC anti-rat emitted green fluorescence which represents conjugated rat IgG with iron particles. In addition, the IgG were also covalently bonded on the Fe–poly(AA)

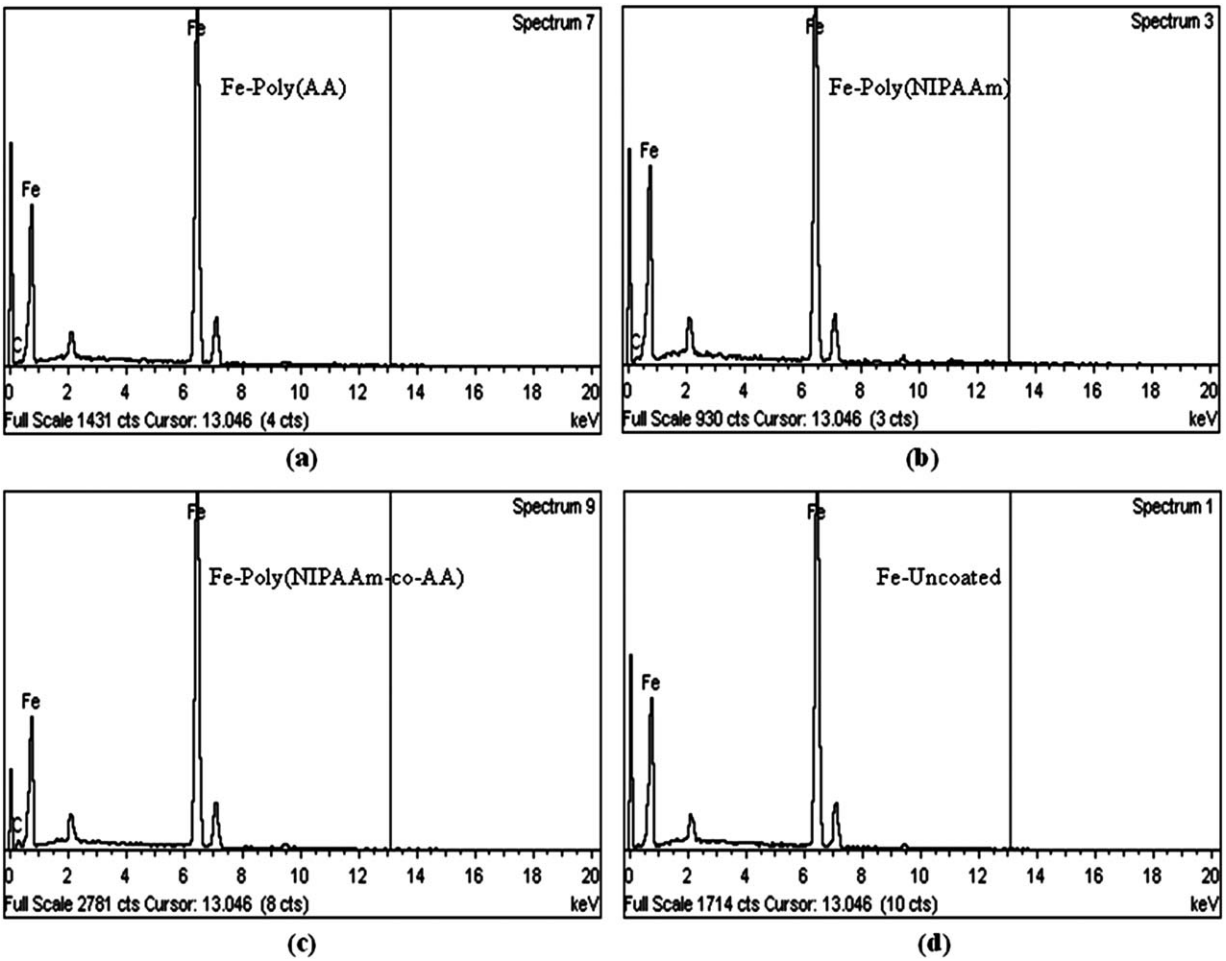

Figure 11. The X–EDS spectrograms of: (a) Fe–poly(AA), (b) Fe–poly(NIPAAm), (c) Fe–poly(NIPAAm-*co*-AA), and (d) Fe–uncoated.

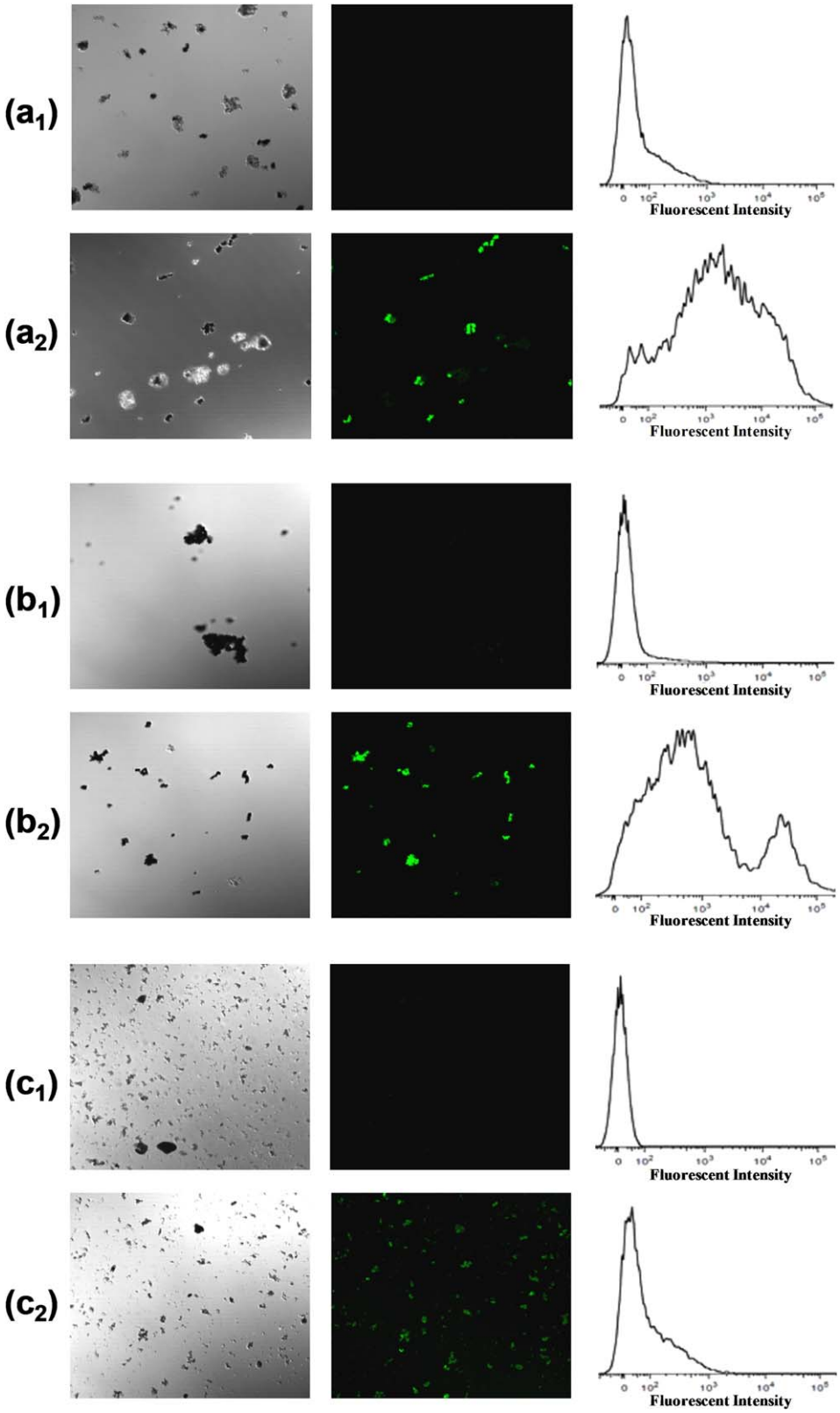

Figure 12. The microscope images in differential interference contrast mode (left), fluorescence mode (middle), and cytometry test result (right) of Fe-polymer-IgG (subscript 1, as a control) and Fe-polymer-IgG-FITC anti-rat (subscript 2, fluorescent labeled). Where: *a* is Fe–poly(NIPAAm-*co*-AA); *b* is Fe–poly(NIPAAm); and *c* is benchmark Fe-COOH. [Color figure can be viewed in the online issue, which is available at wileyonlinelibrary.com.]

and Fe-COOH. From fluorescence images of a_2, b_2, and c_2, the surface polymerized poly(AA) and poly(NIPAAm-*co*-AA) emitted brighter fluorescence than Fe-COOH. However, the brightness on the image a_2 appears not to be uniform which was caused by a low depth of field. On image b_2, two fluorescence intensity distributions which may be caused by the wide range of microsphere sizes where smaller iron particles may be labeled more than larger ones. The cytometry results showed that the fluorescence brightness of microspheres increases 100–1000 times after conjugation with FITC anti-rat. Also, the fluorescence intensity of surface coated iron particles with poly(AA) and poly(NIPAAm-*co*-AA) was 10 times higher than the benchmark Fe-COOH. It may be caused by the amount of acrylic acid functional groups on the polymer which was higher than the benchmark Fe-COOH. As a result, it may become beneficial when surface coated iron particles with poly(AA) and poly(NIPAAm-*co*-AA) are used for protein separation and cell targeting which can bind greater quantities of proteins and cells.

CONCLUSIONS

In this study, we synthesized and characterized multifunctional materials based on micron-size iron particles. The functionalities consist of cell targeting, imaging, drug delivery, and magneto-immune response. ATRP was successfully used as a technique to surface graft polymers on iron particles at mild temperature in the presence of copper (II) bromide. Surface grafting of polymers on iron particles results in a higher glass transition temperature than non-grafted polymers because of the covalent bond which results between the polymer chains and the inorganic substrate which restricts the mobility of the molecules. The surface grafted poly(NIPAAm-*co*-AA) thickness was in the range of 20–50 nm which will not reduce the magnetic saturation of the iron particles. The versatility of targeting bio-molecules was demonstrated by conjugation of rat immunoglobulin to target FITC anti-rat. Fluorescence microscopy and flow cytometry revealed the fluorescence intensity of targeted FITC anti-rat on the iron particles. The iron particle based multifunctional materials are low cost materials for protein separation, drug delivery, and an alternative for hyperthermia and cancer curing agent through magneto-immune response by exposure using magnetic fields.

ACKNOWLEDGMENTS

This research was supported by Department of Defense (DOD-USAMC-MED), grant number W81XWH-09-1-0034. The authors are grateful to Dr. Ravi Subramanian, Chemical and Materials Engineering Department, University of Nevada, Reno, provided FTIR analysis; Dr. Sean M. Ward and a Morphology Core Laboratory supported by COBRE, (NIH/NCRR, 5P20-RR018751) and an equipment grant from the NCRR for the Zeiss LSM510 confocal microscope (1 S10 RR16871) for the collection of microscopic images; Dr. Douglas Redelman, Physiology and Cell Biology Department, University of Nevada, Reno, provided Flow Cytometry analysis; Flow Cytometry analysis supported by INBRE grant (NIH P20 RR016464); Dr. Sujing Xie, CAMCOR University of Oregon, Eugene, provided TEM images.

REFERENCES

1. Jones, S. K.; Winter, J. G. *Phys. Med. Biol.* **2001**, *46*, 385.
2. Gupta, A. K.; Gupta, M. *Biomaterials* **2005**, *26*, 3995.
3. Zhou, L.; Yuan, J.; Wei, Y. *J. Mater. Chem.* **2011**, *21*, 2823.
4. .Available at: http://www.amagpharma.com/products/feridex_iv.php.
5. .Available at: http://www.polysciences.com.
6. Schild, H. G. *Prog. Polym. Sci.* **1992**, *17*, 163.
7. Kotsuchibashi, Y.; Kuboshima, Y.; Yamamoto, K.; Aoyagi, T. *J. Polym. Sci.: Part A: Polym. Chem.* **2008**, *46*, 6142.
8. Wang, J.; Matyjaszewski, K. *J. Am. Chem. Soc.* **1995**, *117*, 5614.
9. Odian, G. Principles of Polymerization, 4th ed.; Wiley: New York, **2004**.
10. Matyjaszewski, K.; Xia, J. *Chem. Rev.* **2001**, *101*, 2921.
11. Kamigaito, M.; Ando, T.; Sawamoto, M. *Chem. Rev.* **2001**, *101*, 3689.
12. Hu, B.; Fuchs, A.; Huseyin, S.; Gordaninejad, F.; Evrensel, C. *Polymer* **2006**, *47*, 7653.
13. Wu, T.; Zhang, Y.; Wang, X.; Liu, S. *Chem. Mater.* **2008**, *20*, 101.
14. Nagase, K.; Kobayashi, J.; Kikuchi, A.; Akiyama, Y.; Kanazawa, H.; Okano, T. *Langmuir* **2008**, *24*, 511.
15. Zhang, H.; Lei, X.; Su, Z.; Liu, P. *J. Polym. Res.* **2007**, *14*, 253.
16. Morinaga, T.; Ohkura, M.; Ohno, K.; Tsujii, Y.; Fukuda, T. *Macromolecules* **2007**, *40*, 1159.
17. Ranjan, R.; Brittain, W. J. *Macromolecules* **2007**, *40*, 6217.
18. Jin, S.; Liu, M.; Chen, S.; Gao, C. *Macromol. Chem. Phys.* **2008**, *209*, 410.
19. Fuchs, A.; Sutrisno, J.; Gordaninejad, F.; Caglar, M. B.; Liu, Y. *J. Appl. Polym. Sci.* **2010**, *117*, 934.
20. Xu, J.; Ye, J.; Liu, S. *Macromolecules* **2007**, *40*, 9103.
21. Zheng, G.; Pan, C. *Polymer* **2005**, *46*, 2802.
22. Xu, F. J.; Kang, E. T.; Neoh, K. G. *Biomaterials* **2006**, *27*, 2787.
23. Wang, X. S.; Armes, S. P. *Macromolecules* **2000**, *33*, 6640.
24. Ning, Y. C. Structural Identification of Organic Compounds with Spectroscopic Technique; Wiley-VCH, Weinheim: **2005** (Appendix 2).
25. Lau, W. S. Infrared Characterization for Microelectronics; World Scientific Publishing: Singapore: **1999**, Chapter *8*.
26. McMurry, J. Organic Chemistry, 4th Ed., Brooks/Cole Pub. Co.: Pacific Grove, **1995**.
27. Maeda, Y.; Higuchi, T.; Ikeda, I. *Langmuir* **2000**, *16*, 7503.
28. Anirudhan, T. S.; Tharun, A. R.; Rejeena, S. R. *Industrial Eng. Chem. Res.* **2011**, *50*, 1866.
29. Hirashima, Y.; Sato, H.; Suzuki, A. *Macromolecules* **2005**, *38*, 9280.
30. Herrera, A. P.; Rodríguez, M.; Lugo, M. T.; Rinaldi, C. *J. Mater. Chem.* **2008**, *18*, 855.
31. Kujawa, P.; Goh, C. C. E.; Calvet, D.; Winnik, F. M. *Macromolecules* **2001**, *34*, 6387.

32. Silverstein, R. M.; Bassler, G. C. Spectrometric Identificcation of Organic Compounds, John Wiley and Sons, London, **1963**, Chapter *3*.

33. Nyquist, R. A. Interpreting Infrared, Raman, and Nuclear Magnetic Resonance Spectra; Academic Press, London, **2001** (Table 11.17A).

34. Li, Y. Y.; Zhang, X. Z.; Cheng, H.; Kim, G. C.; Cheng, S. X.; Zhuo, R. X. *Biomacromolecules* **2006**, *7*, 2956.

35. Hoare, T.; Pelton, R. *Langmuir* **2008**, *24*, 1005.

36. Dong, R.; Krishnan, S.; Baird, B. A.; Lindau, M.; Ober, C. K. *Biomacromolecules* **2007**, *8*, 3082.

37. Chan, C. K.; Chu, I. M. *Polymer* **2001**, *42*, 6089.

38. Tirkistani, F. A. A. *Carbohydr. Polym.* **1997**, *34*, 329.

39. Sousa, R. G.; Magalhaes, W. F.; Freitas, R. F. S. *Polym. Degrad. Stabil.* **1998**, *61*, 275.

40. Garay, M. T.; Alava, C.; Rodriguez, M. *Polymer* **2000**, *41*, 5799.

41. Sutrisno, J.; Fuchs, A.; Sahin, H.; Gordaninejad, F. *J. Appl. Pol. Sci.* **2013**, *128*, 470.

42. You, J. L.; Park, B. J.; Choi, H. J.; Choi, S. B.; Jhon, M. S. Proc. the 10th Intl. Conf. Electrorheological Fluids and Magnetorheological Suspensions (**2006**) 719.

43. Lokander, M.; Stenberg, B. *Polym. Test.* **2003**, *22*, 245.